LOW TEMPERATURE THERMAL CONDUCTIVITY

OF $KMgF_3:Cr^{2+}$

By

AUGUSTO R. LOPEZ

Licenciado
Universidad Pedagogica y Technologica de Colombia
Tunja, Colombia
1962

Master of Science
Emporia Kansas State College
Emporia, Kansas
1969

Submitted to the Faculty of the Graduate College
of the Oklahoma State University
in partial fulfillment of the requirements
for the Degree of
DOCTOR OF PHILOSOPHY
July, 1976

LOW TEMPERATURE THERMAL CONDUCTIVITY

OF $KMgF_3:Cr^{2+}$

Thesis Approved:

George S. Dixon
Thesis Adviser

W. A. Shurcliff

Joel J. Martin

Horacio A. Mottola

Norman N. Durham
Dean of the Graduate College

PREFACE

The study consisted of measuring the thermal conductivities of two undoped and two chromous-doped samples of potassium magnesium fluoride which were grown in the Oklahoma State University Crystal-Growing Laboratory by a Bridgman-Stockbarger technique.

$KMgF_3$ is an insulator which provides an ideal host lattice for the study of paramagnetic impurities, that like Cr^{2+} interacts strongly with the lattice. The results were analyzed in terms of the Debye-Callaway model which incorporated relaxation times resulting from boundary, isotope, phonon-phonon and resonant scattering.

The phonon scattering resonances observed were interpreted in the light of the Fletcher and Stevens model for the Jahn-Teller effect of octahedrally co-ordinated $3d^4$ ions.

The author wishes to express his gratitude to his major advisor, Professor George S. Dixon, for his guidance and assistance throughout this study, as well as his encouragement, personal attention and kindly friendship shown during the author's stay at Oklahoma State University.

Appreciation is also expressed to Professor J. J. Martin for growing the samples, letting us use his laboratory and his assistance. Professor Z. Al-Shaieb who made the atomic absorption spectroscopic determination of the samples impurities. Professors W. A. Sibley and H. Mottola, committee members.

A note of thanks is given to the Department of Physics of Oklahoma

State University; the Universidad Industrial de Santander, Bucaramanga, Colombia; the Icetex of Colombia and the Comision para Intercancambio Educativo for their invaluable collaboration.

TABLE OF CONTENTS

TABLE OF CONTENTS (Continued)

LIST OF TABLES

LIST OF FIGURES

CHAPTER I

INTRODUCTION

Purpose of This Investigation

Thermal conductivity measurements were performed on different samples of nominally pure and chromous-doped potassium magnesium fluoride single crystals. In doing these experiments a threefold purpose was pursued. First, to use thermal conductivity as a spectroscopic tool to determine the energy states of impurities in crystals. Second, to study interactions of transition metal ions with phonons. And third, the possibility exists of driving the Cr^{2+} vibronic states with an external electromagnetic field and generate phonons with energies corresponding to transitions between vibronic energy levels. These will have frequencies $\sim 10^{11}$ Hz and there are presently no good monochromatic phonons generators on this frequency range. Determining the energy states of Cr^{2+} provides a first step toward this application.

Resonant Scattering From Paramagnetic Defects

The interaction between a paramagnetic ion and the vibrations of the lattice in which it is located can be studied by several experimental methods. One of these methods is thermal conductivity, which in a paramagnetic crystal is determined by the average interaction of the thermal phonons with the magnetic ions.

In an insulating paramagnetic crystal, at low temperature only the lowest energy levels of the magnetic ions are populated. The thermal conductivity can be expressed as the sum of contributions from phonons of different energies. The greatest contribution to the heat current is made by phonons with energy near 3.8 KT. At higher and lower energies the distribution falls smoothly to zero. In an ideal insulating crystal this heat current spectrum has its maximum at a phonon energy of 3.8 KT; Orbach (1).

If the difference in energy between a pair of low-lying energy levels happens to be comparable to the energy of the dominant phonons, then phonons may induce transitions in the magnetic ions. In doing so, the phonons will themselves be scattered, because of their absorption and subsequent re-emission in random directions. This reduces their contribution to the heat current and produces an increase in the thermal resistivity of the specimen. The phonons which are at resonance with the energy levels of the magnetic ions are prevented from contributing to the heat current (2,3,4).

Cr^{2+} in Octahedral Sites

Cr^{2+} is a $3d^4$ ion and interact strongly with the lattice, particularly when it is in an octahedral site.

In an octahedral environment the ground state orbital level of Cr^{2+} should be ^5E. However, the Jahn-Teller theorem indicates that the orbital degeneracy will be removed by spontaneous lower symmetry distortions of the surroundings (5).

The Jahn-Teller effect in octahedral symmetry leads to vibronic states for the chromous ion and nearest neighbor octahedrals. This is

an extended defect and can interact with the phonons that carry heat in the crystal, so one may expect resonant scattering of phonons from the vibronic states of the complex. Fletcher and Stevens (6) developed a model for the dynamical Jahn-Teller effect of octahedrally coordinated $3d^4$ ions to apply to experimental results of acoustic paramagnetic resonance with $MgO:Cr^{2+}$. This model has been used also by Challis (7) to account for the resonances in thermal conductivity measurements in $MgO:Cr^{2+}$.

According with this model of Fletcher, the ground state of a $3d^4$ ion splits into seven energy levels A_1, A_2, E_1, E_2, T_2 and T_2'. By group theory selection rules only eight transitions are allowed: $E_2 - A_1$, $E_1 - A_1$, $A_2 - E_2$, $E_1 - E_2$, $E_1 - A_2$, $T_2' - T_1$, $T_2 - T_1$ and $T_2 - T_2'$. The energy levels from this model depend mainly of two parameters: δ, the tunneling frequency and D, the spin-orbit coupling. The energy level E_1, for example has the form

$$E_1 = \frac{\delta}{6} + \left(\frac{\delta^2}{4} + 2f_2{}^2 D^2\right)^{\frac{1}{2}} \qquad (1)$$

Expressions for all energy levels are presented in Appendix G.

Lange and Guha have also used this model in their acoustic paramagnetic resonance experiments on MgO:Cr and $KMgF_3$:Cr (8,9).

CHAPTER II

EXPERIMENTAL PROCEDURE

Properties of $KMgF_3$

Potassium magnesium trifluoride is a cubic perovskite insulator compound with one molecule per unit cell and a lattice constant of 3.973Å (10). Its structure is shown in Figure 1, and its elastic constants C_{11}, C_{12} and C_{44} have been determined from ultrasonic experiments (11). The density of $KMgF_3$ is 3.17 ± 0.01 gm/cm^3, calculated from the lattice parameter, and its average velocity of sound reported (12) is 4.77 x 10^5 cm/sec. $KMgF_3$ has a relatively low melting-point, 1340K, that makes it possible to grow crystals from small quantities of high purity starting materials.

Growth of the Samples

The undoped and chromous doped samples of potassium magnesium fluoride were grown in the Oklahoma State University Crystal Growth Laboratory from stoichiometric mixtures of KF and MgF_2 by a Bridgman-Stockbarger technique. Time needed to grow the $KMgF_3$ crystal was about one week. Dopant Cr was added by adding CrF_2 to the melt. Detail about the growth apparatus and procedure is given by Wolf (13).

Preparation of Samples

Thermal conductivity specimens were cut from the single crystals

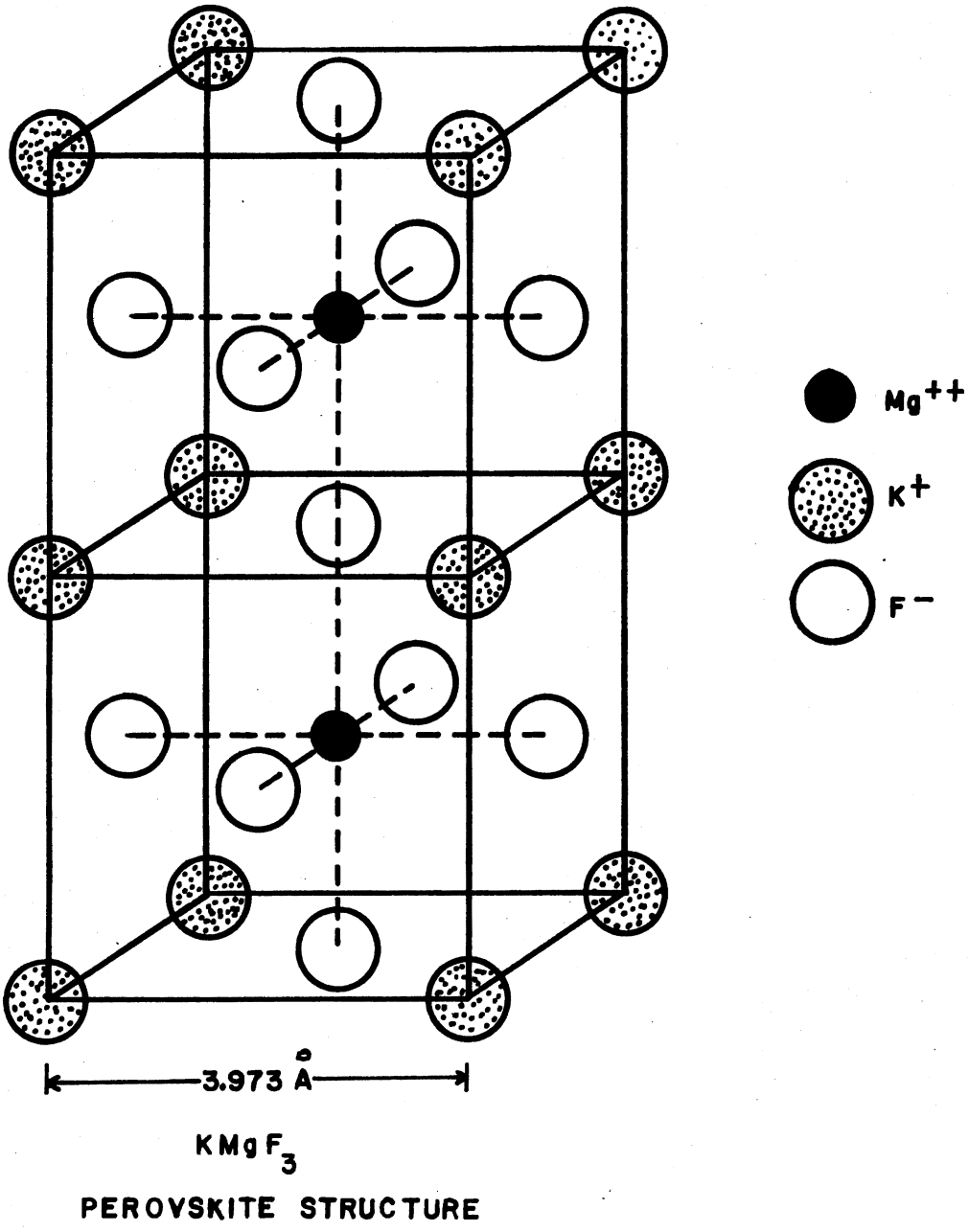

Figure 1. Crystal Structure of Potassium Magnesium Fluoride

in the form of rods. Samples C and D were cut with the [110] and [100] axis respectively along the length. The concentration of chromous impurities in the crystal was determined by the atomic absorption spectroscopic method in the Oklahoma State University laboratory of Professor Z. Al-Shaieb. The measured concentrations were probably accurate to about ±20%. Dimensions and Cr concentration of samples appear in Table I.

Experimental Determination of Thermal Conductivity

The thermal conductivities of the samples were measured by the steady-state heat flow method. This method is very well known and extensively found in the literature. Nevertheless a short review is given. In this method the thermal conductivity, λ, for a solid with a steady-stay flow of heat is defined by the relation

$$\lambda = Q/|\nabla T| \tag{2}$$

where Q is the energy transmitted across unit area per unit time and ∇T is the temperature gradient. Equation (2) becomes

$$\lambda = \frac{P}{A}\frac{L}{\Delta T} \tag{3}$$

where P is the power supplied to one end of the sample, L is the distance between which the change in temperature ΔT is measured, that is the thermometer separation, and A is the cross section of the sample.

Apparatus

For the range of temperature 2.3 to 150^{o}K in which the measurements

TABLE I

DIMENSIONS OF SAMPLES

	Sample	Cross Section (mm^2)	Orientation	Cr^{2+} Concentration (μmole/mole)	Boule
A	$KMgF_3$:undoped	19.27	random	---	061674
A1	$KMgF_3$:undoped	5.06	random	---	061674
B	$KMgF_3$:Cr-doped	6.35	random	50	081374
D	$KMgF_3$:Cr-doped	11.78	[100]	100	022475
C	$KMgF_3$:Cr-doped	9.46	[110]	100	022475

were performed, an apparatus described in considerable detail by Wolf (13), was used. Figure 2 shows an schematic of the sample holder. The sample was mounted at the end of a copper rod which was constructed so that the effective thermal contact with the cryogenic liquid bath, either liquid helium-4 or liquid nitrogen, could be controlled by controlling the pressure of helium gas in the heat leak chamber. When helium gas was put into this chamber, the thermal contact with the cryogenic bath was good, giving the copper rod the same temperature as the bath. If the sample was heated and transmitted heat to the copper rod or if a current was passed through the 100 ohm ambient heater wrapped around the copper rod, the heat was quickly dissipated into the bath, approximately maintaining the bath temperature. If the thermal contact between the copper heat sink and the cryogenic bath was reduced by pumping some of the helium gas out of the heat leak chamber, then the heat dissipated to the copper heat sink was not removed efficiently and raised the temperature of the heat sink and sample. With a good vacuum in the heat leak chamber, the heat sink was effectively isolated from the cryogenic bath; therefore, temperatures much higher than the bath's could be reached. If the cryogenic liquid was helium-4 at 4.2K, temperatures as high as 50K could be reached with less than 250 milliwatts of input power. If liquid nitrogen at 77K was the cryogenic liquid, temperatures above 200K could be obtained with approximately one watt of input power. At the higher temperatures, radiation loss became a large source of error when the sample temperature was greatly different from that of the outer wall of the sample holder. For reduction of this radiation loss, an aluminum heat shield was placed around the sample, its clamps, and its gradient heater. This aluminum shield was in thermal

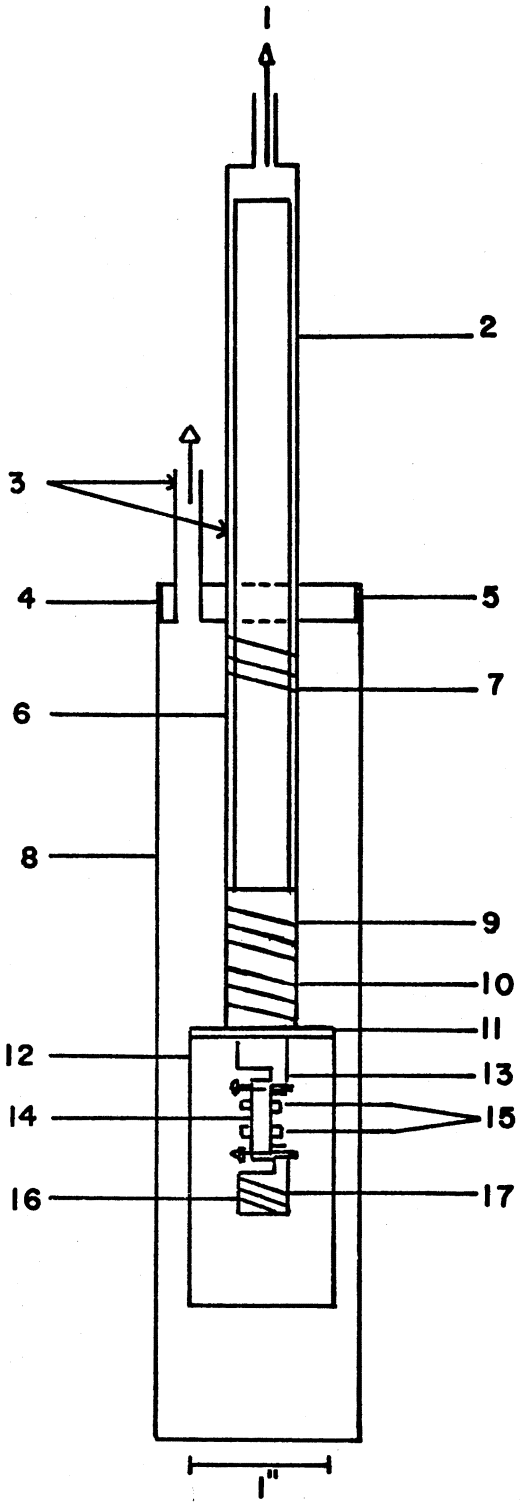

1-TO VACUUM PUMP OR HELIUM GAS
2-VARIABLE HEAT LEAK CHAMBER
3-STAINLESS STEEL TUBING
4-BRASS
5-VACUUM SEAL
6-COPPER HEAT SINK
7-SAMPLE LEADS
8-BRASS CAN
9-AMBIENT HEATER
10-SAMPLE LEADS
11-ALUMINUM WASHER
12-ALUMINUM CAN
13-SAMPLE CLAMP
14-SAMPLE
15-THERMOCOUPLE CLAMPS
16-COPPER BLOCK
17-GRADIENT HEATER

Figure 2. Thermal Conductivity Sample Holder

contact with the copper heat sink rod and was therefore kept at approximately its temperature, greatly reducing the temperature difference between the sample and its surroundings. The entire assembly described above was enclosed in a brass can which was then submerged into the cryogenic fluid.

When measurements were being taken, a pressure of less than 10^{-5} Torr was maintained inside the brass can, thus insuring proper temperature and heat loss control. The sample was held in thermal contact with the heat sink by a copper clamp containing indium pads which flattened against the sample when the nylon screws were tightened. A phosphor bronze spring and the nylon screws compensated for the difference in the thermal expansion between the sample and the clamp. The two thermometer clamps were constructed in a similar manner.

In samples A and A1, the temperature gradient was established by a heater wound around the end of the sample farthest from the heat sink. Samples B, C and D had the heater clamped onto the end of it. Current was supplied to the heaters by #40 copper wires and the voltage drop across the heaters was measured through #36 constantan wires.

The thermometers used in this apparatus were chromel versus gold 0.07 atomic percent iron thermocouples soldered to the clamps with indium solder so that the emf of T and ΔT was read directly using a potentiometer.

T and ΔT were measured with a Leeds and Northrup type K-3 universal potentiometer, a Model 2770 Honeywell potentiometer and a Leeds and Northrup 9838 guarded nanovolt detector as described by Wolf (13) as well as the thermocouple calibration involved in the thermometry.

Errors

The dimensions used to calculate the cross-section A were measured with a micrometer to the nearest .01 mm. None of the samples was a perfect parallelepiped so averages values were used. The measurement of the thermometer spacing, L, was the most uncertain measurement taken. It was performed by placing a spacer between the middles of the thermometer clamps or between the inner edge of one clamp and the outer one of the other clamp; then the thickness was measured with a micrometer.

The above measurements of the cross-sectional areas and the clamp separations were made only once for each sample during a particular data run, therefore the uncertainties in these measurements remained constant and did not affect the shape of the thermal conductivity curve.

The input power to the hot end of the sample was calculated by using $P = IV$. The current I was determined by measuring the voltage drop across a 10 ohm standard resistor, read from a digital millivoltmeter. The voltage V was read directly from the digital millivoltmeter.

Direct use of Equation (2) assumes that all the power that was calculated converted to heat that flowed uniformly through the sample. Dissipation of heat due to convection and conduction directly from the sample to the wall of the sample holder was ruled out since the sample was in a vacuum of better than 10^{-5} Torr. Consideration of conduction through the wire leads going into the sample chamber for this particular apparatus was analyzed by Wolf (13) and dissipation of heat due to conduction was found to be negligible.

The radiation heat loss, $Q_{RADIATION}$, was approximated by using the Stefan-Boltzmann law

$$Q_{RADIATION} = 4S\sigma ET^3\Delta T \qquad (4)$$

where S is the surface area of the sample, σ is the Stefan-Boltzmann constant, E is the emissitivity of the sample, T is its temperature and ΔT is the difference between the sample's temperature and the chamber wall's temperature. At low temperatures the radiation heat loss was negligible, but at higher temperatures, 150 to 200K, it could become quite significant. As an example for 150 and 200K the radiation heat loss was calculated to be 22 and 87 mW respectively, by using Equation (4), with S for the largest sample, A, equal 391 mm^2, and assuming E as its maximum possible value, that is one. Those values found for Q_R were larger than the maximum input power used, some 15 mW. To allow data to be taken at 150 or 200K the sample chamber was surrounded with an aluminum can as discussed in the section describing the apparatus. With the aluminum can heat shield, which attained a temperature close to that of the upper termometer attached to the sample a heat loss of less than 1 mW could be expected for a ΔT of the order of the temperature difference between the two thermometers attached to the sample and that was of the order of 0.2K for T equal 150K.

CHAPTER III

EXPERIMENTAL RESULTS

The thermal conductivities of two undoped samples and three chromous-doped samples of potassium magnesium fluoride single crystals were measured from 2.4 to 150^{o}K. On the undoped sample with smaller cross section a few measurements were taken from 3.8 to 80^{o}K. The data between 2.4 and 150^{o}K for all samples is presented in Figure 3.

The shapes of the curves for the undoped samples were characteristic for single-crystal insulating materials. For temperatures above 50K the thermal conductivities for all the samples were the same, having the characteristic slope of T^{-1} resulting from the dominance of phonon-phonon interactions. In the peak region between 18 and 25K, the thermal conductivities of sample A had a higher peak, approximately 6 and 7 W/cmK difference with respect to samples B, C and D. Below 4K the thermal conductivity curve of sample A had a slope of approximately T^{3}. The conductivity of the doped samples B, C, and D had a depression at about 3K.

In the Debye-Callaway approximation (14), λ/T^{3}, thermal conductivity divided by temperature to the third power, is proportional to a weighted average of the phonon relaxation time; see Equation (5). A curve of λ/T^{3} versus T, from 2.3 to 12K is shown in Figure 4 for samples B and C. These plots show a pronounced depression in λ/T^{3} about 3K in both doped samples and a peak about 7K. These indentations in λ/T^{3} con-

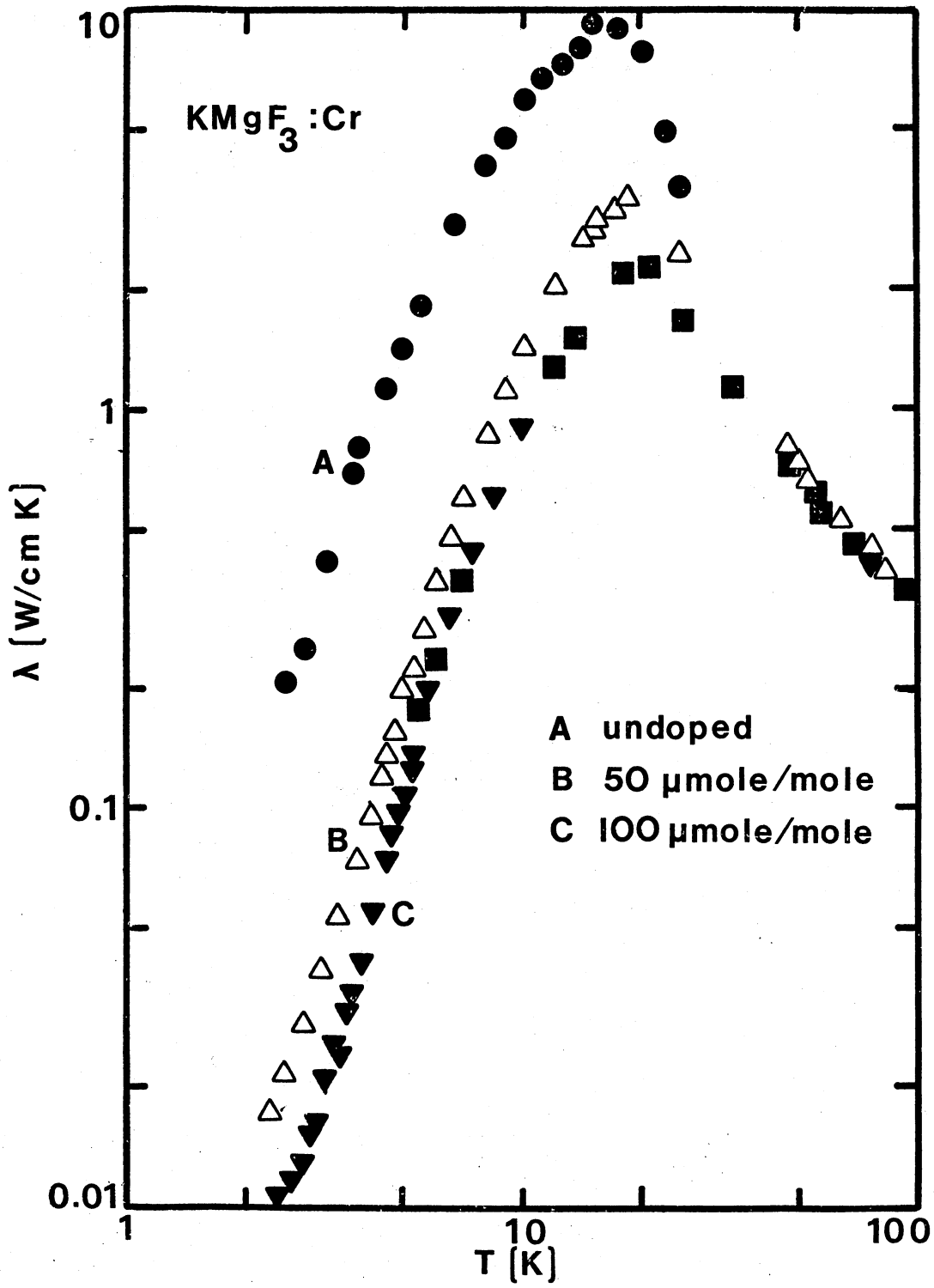

Figure 3. Measurements of the Thermal Conductivity of $KMgF_3$

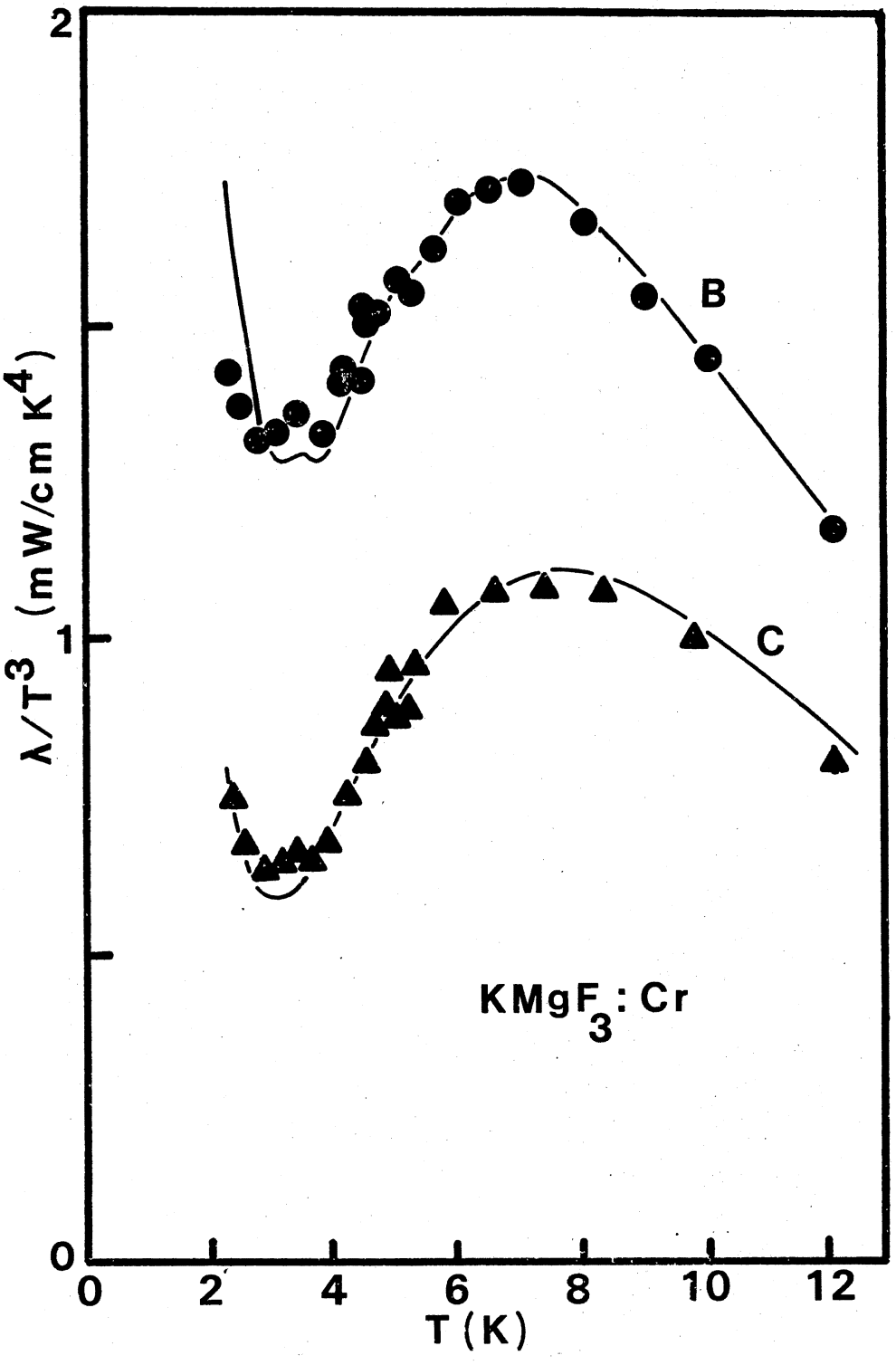

Figure 4. λ/T^3 for Cr-doped Samples of $KMgF_3$

firmed the observation on Figure 3 λ vs T. This particular reduction in the conductivity was interpreted as a resonance. In Figure 4 is also observed a shoulder about 5K in sample B, and a plateau from 6 to 8K in sample C. These shoulder and plateau were also interpreted as evidence of a second higher frequency resonance.

A plot of λ/T^3 vs T for the undoped sample A is shown in Figure 5.

A tabulation of all data points taken is presented in Appendixes A to E.

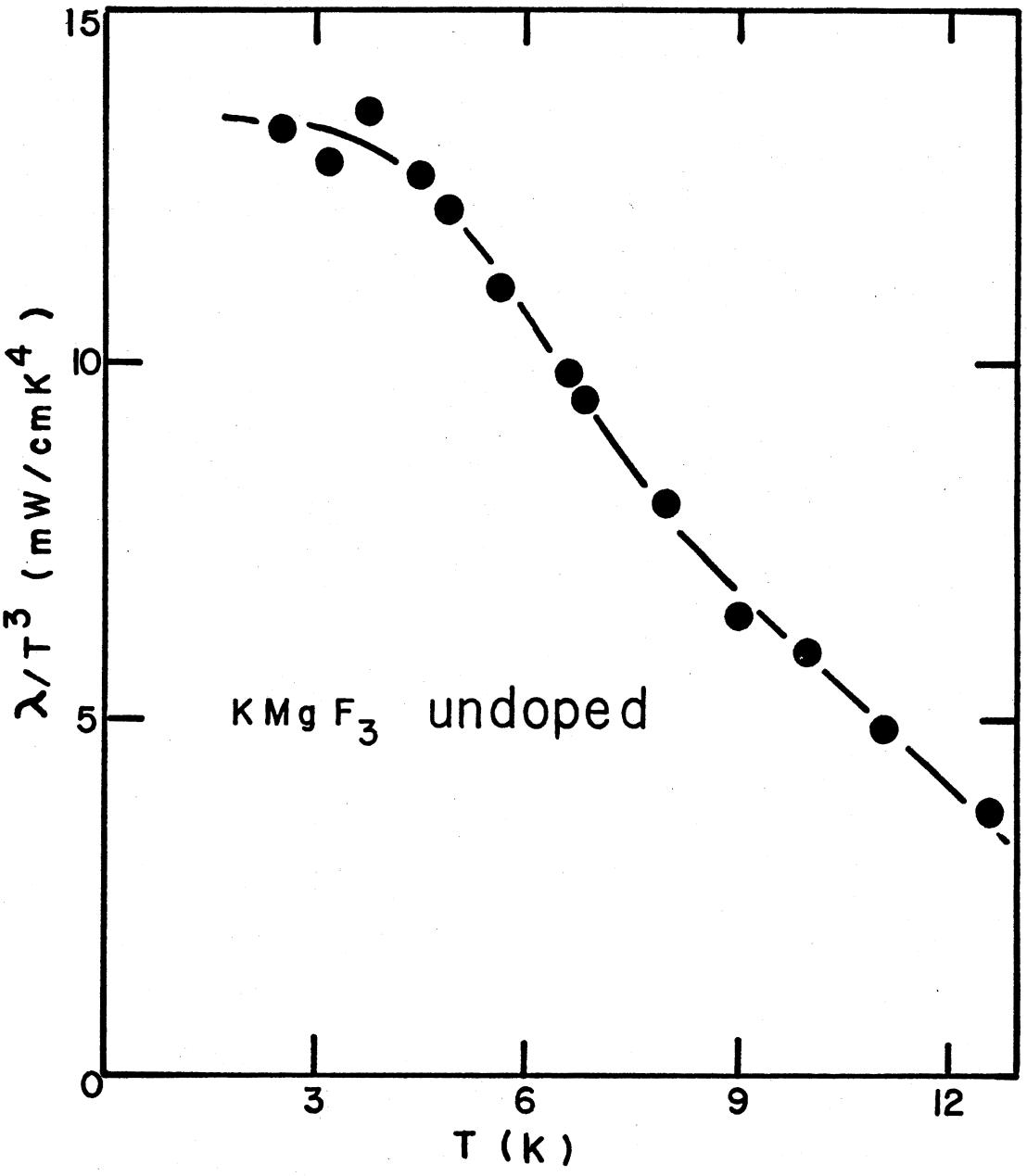

Figure 5. λ/T^3 for $KMgF_3$ Undoped Sample

CHAPTER IV

DISCUSSION AND CONCLUSIONS

Thermal Conductivity of Insulators

Previous experiments have successfully tested the Debye-Callaway model of thermal conductivity (7,14,15,16).

According to the Debye-Callaway model the thermal conductivity, λ, of an insulator is given by

$$\lambda(T) = \frac{k}{2\pi^2 v}\left(\frac{kT}{\hbar}\right)^3 \int_0^{\theta/T} \frac{x^4 e^x}{(e^x-1)^2}\,\tau(x,T)\,dx \qquad (5)$$

$$\left(x = \frac{\hbar\omega}{kT}\right)$$

where v is the sound velocity assumed constant, $\tau(\omega,T)$ is the phonon relaxation time, θ the Debye temperature and the other symbols have their usual meaning.

From Equation (5) it is seen that the thermal conductivity is proportional to a known weighted average of the total phonon relaxation time $\tau(\omega,T)$ which in turn depends on the nature and concentration of the impurities present.

The relaxation time is given by

$$\tau_{TOTAL}^{-1} = \sum_i \tau_i^{-1} \qquad (6)$$

where τ_i are the relaxation times describing the individual scattering sources, assuming the scattering processes are independent of each other. The validity of combining the individual relaxation times by the Equation (6) has been investigated both experimentally and theoretically (2,14,17). At the temperatures of interest in this work, Equation (6) appears to be a consistent way to combine the effects of different scattering processes (2,18). Boundary, point defect and phonon-phonon relaxation times are the most important processes in pure crystals.

A Debye temperature, θ, of 356K was calculated from the equation

$$\theta = \frac{\hbar v}{k} \left(\frac{6\pi^2 N}{V}\right)^{1/3} \tag{7}$$

where N/V is the number of atoms per unit volume in the crystal and v is the velocity of sound.

Discussion and Conclusions

The thermal conductivities above the maximum were the same for all the samples measured, confirming that in this region the phonon-phonon interactions were the dominant scattering mechanisms.

Using Equation (6) in Equation (5) the unknown relaxation times can be determined by curve fitting. For the large temperature range of thermal conductivity measurements for the pure sample A, the best fitting was obtained by assuming three relaxation times: boundary, isotope, and phonon-phonon, such that Equation (6) becomes

$$\tau_{total}^{-1} = \tau_{boundary}^{-1} + \tau_{isotope}^{-1} + \tau_{phonon\text{-}phonon}^{-1} \tag{8}$$

For $\tau_{boundary}$ we used the relation first derived by Casimir (19), re-

sulting from diffuse boundary scattering

$$\tau_B^{-1} = \frac{v}{L} \tag{9}$$

where v is the velocity of sound in the crystal and L is an effective sample diameter which is dependent upon the sample's geometry and is given by

$$L = 2\pi^{-\frac{1}{2}} S^{\frac{1}{2}} \tag{10}$$

where S is the sample's cross section perpendicular to the heat flow.

At low enough temperatures, when all the phonon mean free-paths are comparable to the sample's cross-sectional dimensions, the relaxation time is usually entirely limited by the boundary scattering, which is temperature and frequency independent, so it is expected that the thermal conductivity curve, log-log plot, for these temperatures will have a slope of T^3 resulting from the temperature dependence of the specific heat. This result can be observed in Figure 3. The effective Casimir lengths for all samples are given in Table II. Point defect scattering relaxation time, τ_{PD}, was estimated for the effect of isotopes by using the relation found by Klemens (20), assuming a Rayleigh-type scattering of the phonons. This relaxation time is

$$\tau_{PD}^{-1} = A\omega^4 \tag{11}$$

where

$$A = \frac{\delta^3 \Gamma}{4\pi v^2} . \tag{12}$$

Here δ is the cube root of atomic volume, Γ is a dimensionless

TABLE II

CALCULATED CASIMIR LENGTHS FOR THE SAMPLES

Sample	Boule	Effective Casimir Length $L = 2\pi^{-\frac{1}{2}} S^{\frac{1}{2}}$ (cm)
A	061674	0.495
Al	061674	0.254
B	081374	0.284
D	022475	0.387
C	022475	0.347

parameter and v the average sound velocity.

Various forms of Γ have been suggested (17,21). The form suggested by Slack (22) that may be applied to compound containing isotopes of many elements was used. For a compound with the general form $A_x B_y C_z$, the form of Γ is

$$\Gamma = \frac{x}{x+y+z} \left(\frac{M_A}{\bar{M}}\right)^2 \Gamma_A + \frac{y}{x+y+z} \left(\frac{M_B}{\bar{M}}\right)^2 \Gamma_B + \frac{z}{x+y+z} \left(\frac{M_C}{\bar{M}}\right)^2 \Gamma_C \qquad (13)$$

where

$$\Gamma_A = \sum_i f_i \left(\frac{\Delta M_i}{\bar{M}_A}\right)^2, \ldots\ldots \qquad (14)$$

M_A and M_B are the masses of the isotopes of the atoms of type A and B respectively, $\bar{M}_A$, and $\bar{M}_B$ are the average masses of these atoms, and $\bar{M}$ is the average molecular mass defined as

$$M = \frac{x \bar{M}_A + y \bar{M}_B + z \bar{M}_C}{x + y + z} \qquad (15)$$

f_i is the fractional concentration of the ith isotope and ΔM_i is the difference between atomic mass of the ith point defect, isotope, and the average atomic mass.

Relating the form $A_x B_y C_z$ to K Mg F_3, x = 1, y = 1, z = 3, A = potassium, B = magnesium, and C = fluoride. The approximation for the constant A of Equation (12) using Equation (13) was 1.13×10^{-44}. The details of this calculation are given in Appendix F.

The relaxation time, τ_{PP}, resulting from the phonon-phonon process (23,24) was:

$$\tau_{PP}^{-1} = (BN + BU\, e^{-\theta/aT})\, \omega^2 T \qquad (16)$$

where BN, BU and a are fitted parameters.

With the aid of an electronic computer and the relaxation time

$$\tau^{-1} = \frac{v}{L} + A\omega^4 + (BN + BU\, e^{-\theta/aT})\, \omega^2 T \qquad (17)$$

a good fit of the thermal conductivities data was obtained for the pure sample A. A plot of the experimental and fitted data for this sample appears in Figure 6. The fitted parameters for this sample are given in Table III.

TABLE III

PARAMETERS USED IN THE DEBYE-CALLAWAY INTEGRAL FOR SAMPLE A ($KMgF_3$:UNDOPED)

L(mm)	A(Sec^3)	BN(Sec/K)	BU(Sec/K)	a
0.75	1.1299×10^{-45}	2.5×10^{-20}	6.0×10^{-18}	3.4

The fitted values for the Casimir length L, was almost seven times smaller than the calculated value. This difference could be attributed to bubbles, grain boundaries and trace of magnetic impurities. Harley and Rosenberg (12) in their experiment on thermal conductivity of nickel-doped samples of potassium magnesium fluoride explained the reduction in their Casimir length by considering that the crystals con-

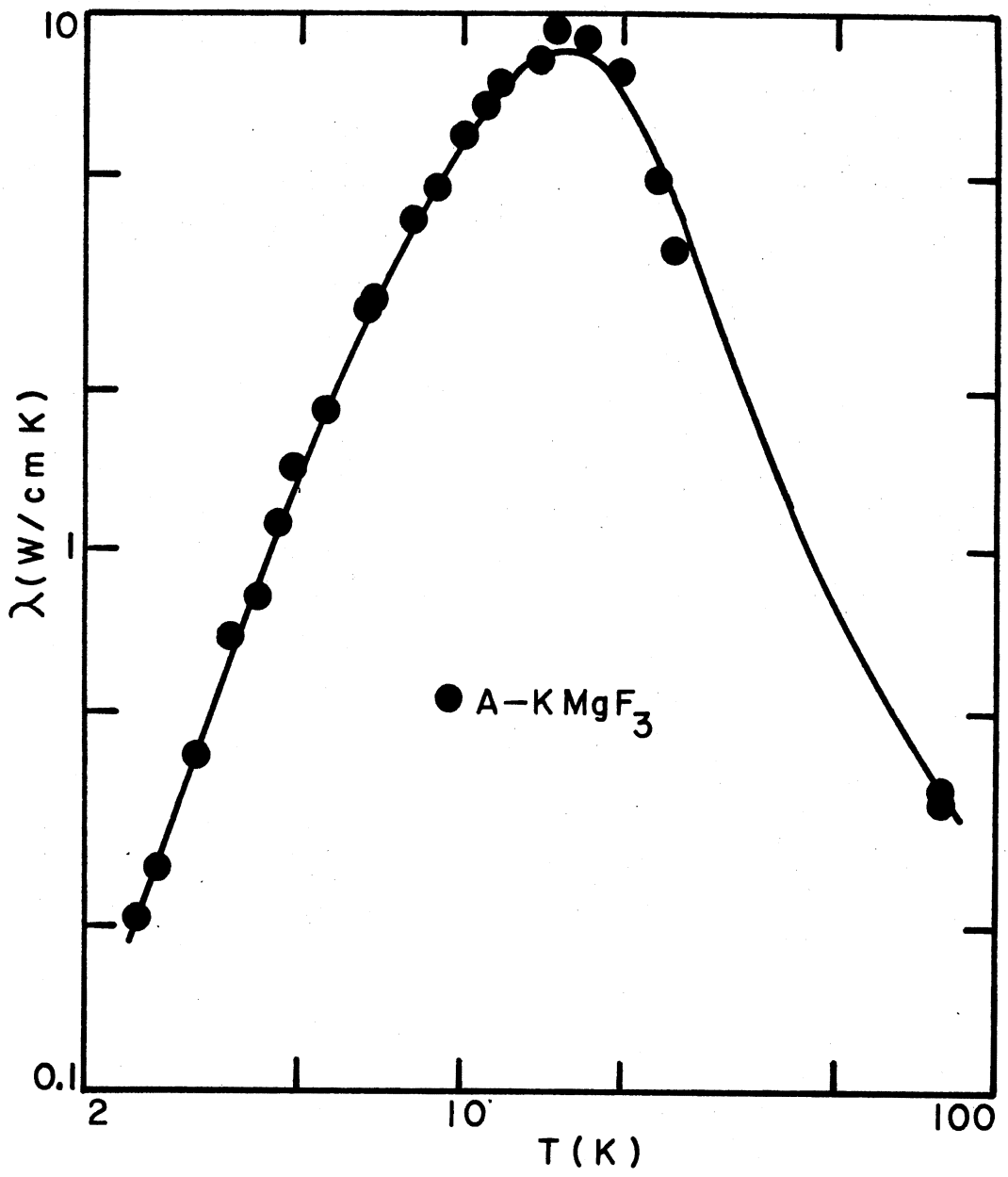

Figure 6. A Comparation of the Measured Thermal Conductivities of $KMgF_3$ With Theoretical Curve Calculated From the Callaway Model

tained some "macroscopic defects". To the present it was not possible to decide which of those possibilities was the correct one for this experiment.

The fitted value for the Rayleigh scattering parameter A was 10 times smaller than the calculated value from Equation (12). This difference was interpreted as due to additional scattering defects.

For our second pure $KMgF_3$ sample A1, the cross section perpendicular to the heat flow was reduced by a factor of 3.8. The thermal conductivities of samples A and A1, versus temperature from 3.8 to 10K are plotted in Figure 7. The experimental data for sample A1 are displayed in Appendix B. For 3.8K the thermal conductivity of the smaller sample was 1.75 times smaller than for sample A. The square root of the ratio of the cross sections was 1.9 showing that at low temperature, below 4K, the Casimir relaxation time appears to be important.

Samples B, C and D were $KMgF_3:Cr^{2+}$, doped samples, whose concentrations are shown in Table I. Samples C and D were both cut from the same boule, but along different crystal planes, [110] and [100] respectively. Their thermal conductivities are plotted in Figure 8, showing no major differences, as expected from a cubic crystal. So the analysis was concentrated in samples B and C whose thermal conductivities are plotted in Figure 9. A careful examination of these graphs shows some indentations in the thermal conductivities about 3K and perhaps about 3.8 or 4K. At liquid nitrogen temperatures, the conductivities were the same, but at the peak, and below, the conductivities were smaller for the more heavily doped sample. At the peak the conductivity was 1 W/cm K smaller in Sample C than in Sample B. On the other hand the thermal conductivities of the chromous-doped samples were considerably smaller, at the

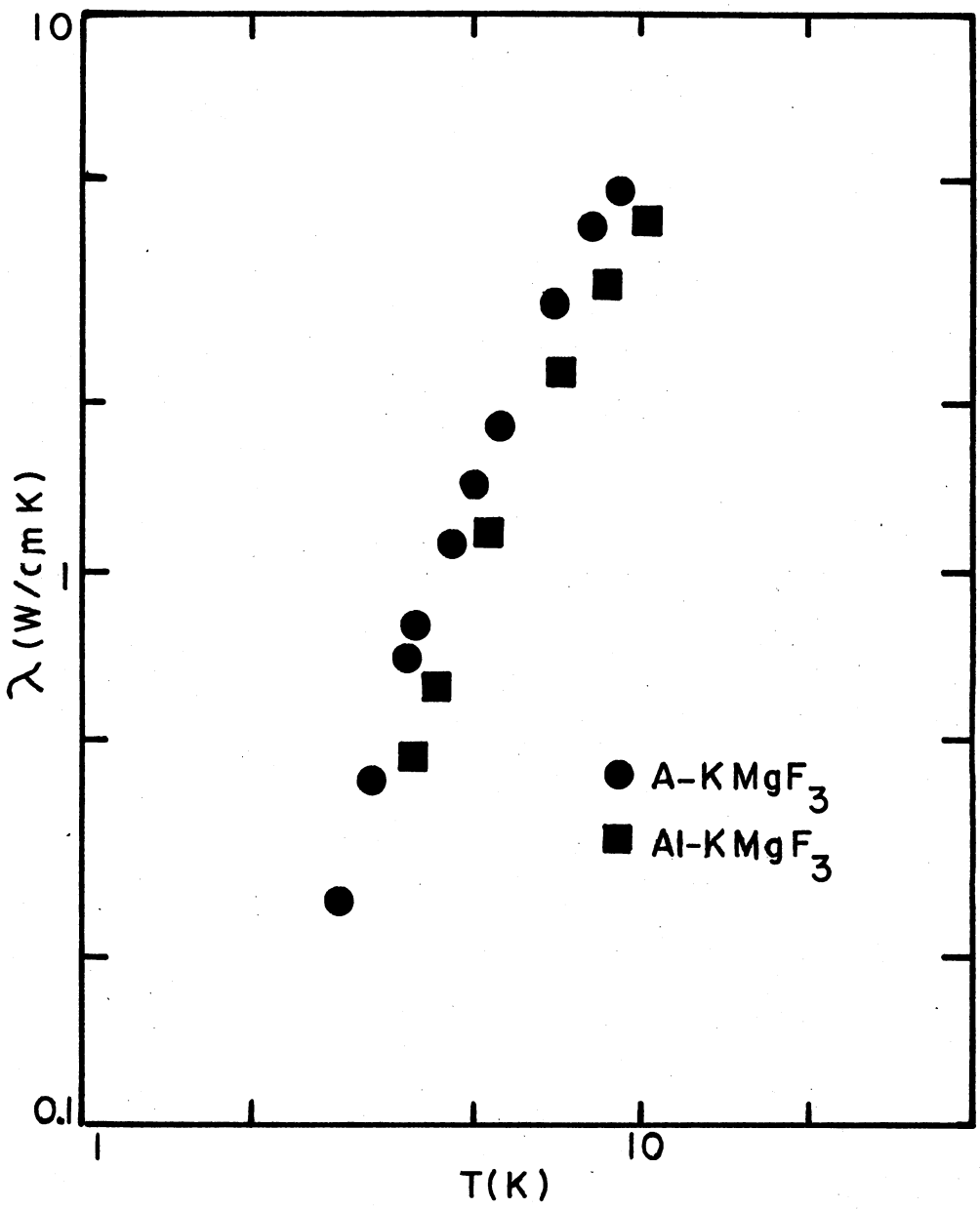

Figure 7. Thermal Conductivity of $KMgF_3$:Undoped Samples

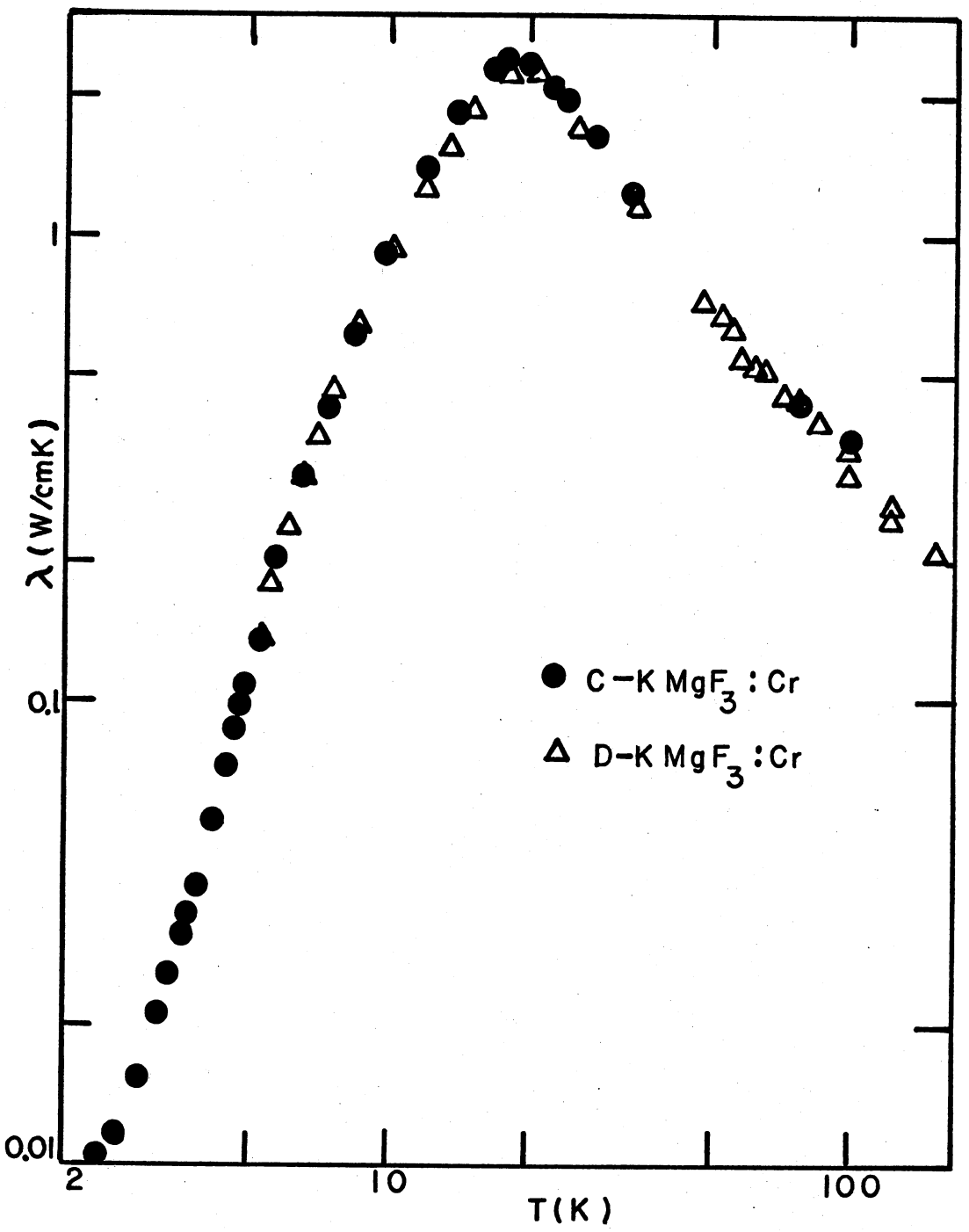

Figure 8. Thermal Conductivity of Cr-doped $KMgF_3$ Samples From Same Boule

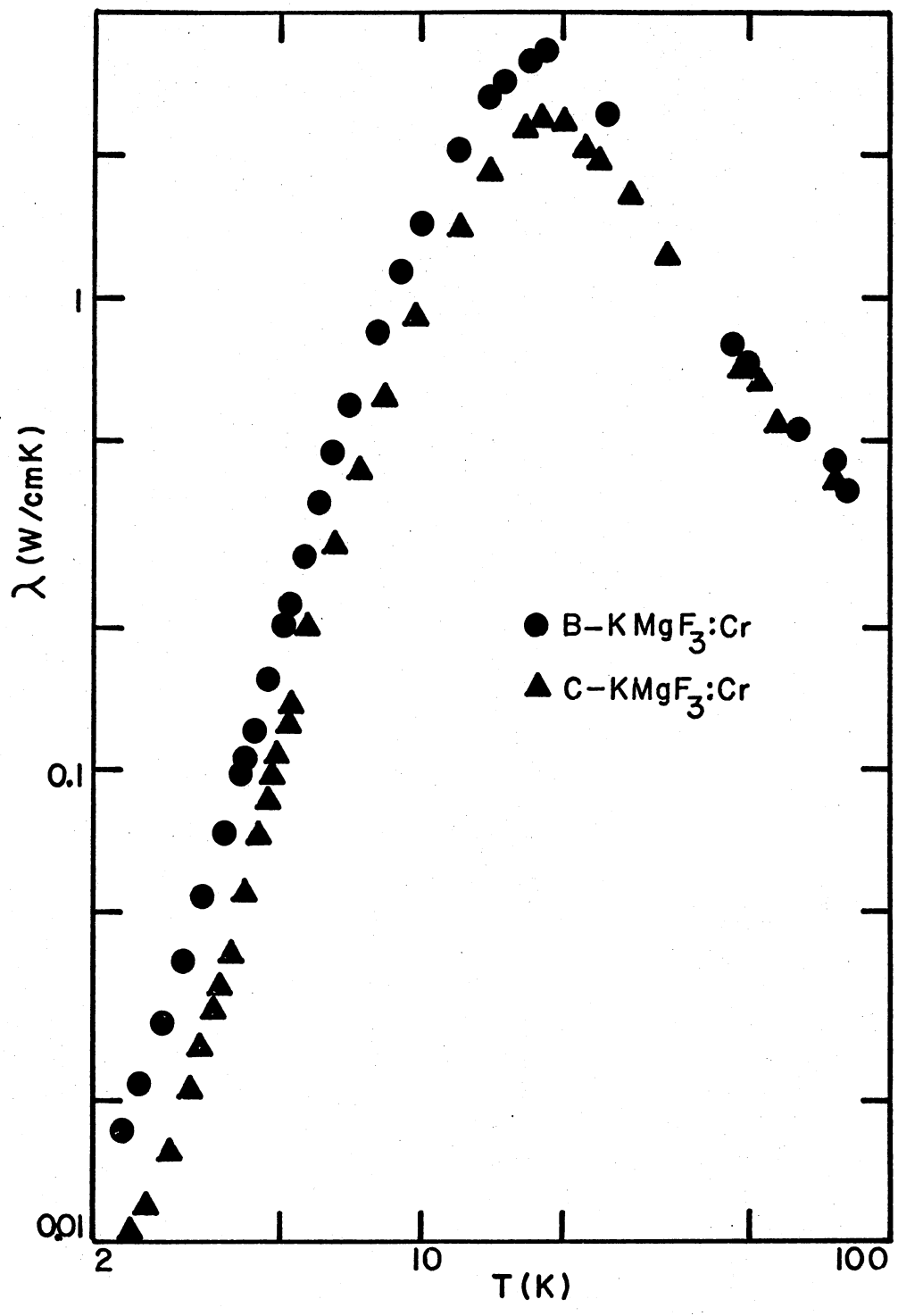

Figure 9. Thermal Conductivity of Cr-doped $KMgF_3$ Samples

peak and below, than in the pure sample A. Three times smaller at the peak and one order of magnitude smaller at 2.5K.

As pointed out in Chapter III, in the Debye approximation λ/T^3 is proportional to a weighted average of the phonon relaxation time. In Figure 4 this quantity is plotted against temperature for samples B and C and in Figure 5 for sample A. If there were only boundary scattering, λ/T^3 would be independent of temperature. This seems to be the case at the lower temperatures in Figure 5 for the pure sample. The low temperature data would be consistent with a resonant scattering process in which the weighted relaxation time falls to a minimum when the dominant phonon frequency equals the resonant frequency and then rises when the dominant phonon increases. Figure 4 shows a pronounced minimum in λ/T^3, that is characteristic of resonant scattering, at about 3K for samples B and C. In the same graph a shoulder at about 5K in sample B is observed, as well as a plateau in λ/T^3 from 6 to 8K, in sample C. These are reduction in λ/T^3 that were interpreted as indicating a second scattering resonance at higher frequency. Beyond 8K, λ/T^3 continues to decrease for both samples B and C.

To account for the data on the chromous doped samples a total relaxation time of the form

$$\tau^{-1} = \tau_P^{-1} + \Delta A\omega^4 + \tau_R^{-1} \qquad (18)$$

was used. Here τ_P is the relaxation time found for the undoped sample. The $\Delta A\omega^4$ is included for the increased Rayleigh scattering expected from the Cr impurities, and τ_R is the resonance relaxation time needed to account for the structure in λ/T^3. For strongly coupled ions, such

as Cr^{2+}, the most important effects on the thermal conductivity come from the wings of the resonance absorption line rather than near the center frequency, ω_o, of the absorption. This is because those phonons with frequencies very close to ω_o are so strongly scattered that they make a negligible contribution to the total heat transport. Thus the choice of the form for the resonant relaxation time can have an influence on the apparent center frequencies of the resonances. Several forms for resonant relaxation times have been suggested in the literature. To choose among these the following criteria were used:

1. The resonance terms should reproduce the λ/T^3 results as closely as possible.

2. The strength of the scattering should scale with the Cr concentration from one sample to another.

3. The number of unknown parameters in the resonance terms should be kept to a minimum.

Two different trial functions for the resonance relaxation time were used. The first

$$\tau_R^{-1} = \frac{B_1 \omega^2}{(\omega_{o1}^2 - \omega^2)^2} + \frac{B_2 \omega^2}{(\omega_{o2}^2 - \omega^2)^2} \qquad (19)$$

was first proposed by Pohl and co-workers to account for resonances due to tunneling defects (25). Recently, Sheard (26) has placed this on a firmer theoretical basis as the appropriate form for scattering in the wings of strong resonances. The second

$$\tau_R^{-1} = \frac{B_1 \omega^4}{(\omega_{o1}^2 - \omega^2)^2} + \frac{B_2 \omega^4}{(\omega_{o2}^2 - \omega^2)^2} \qquad (20)$$

was first derived by Griffin and Carruthers (27) to account for scattering by bound donor electrons in semiconductors. It has also been applied to the paramagnetic defect problem. In both these forms two resonances with center frequencies ω_{o1} and ω_{o2} and coupling strengths B_1 and B_2 are assumed.

The λ/T^3 data for samples B and C suggested that the resonant term had most effect at about 3K. Assuming the dominant phonons have an energy about 3.8 KT, this indicated that ω_{o1} or ω_{o2}, was about 8 cm^{-1}. Values for ω_{o1} between 6 and 12 cm^{-1} were tried for various values of B_1, B_2, ΔA and ω_{o2}. No good fit of the λ/T^3 data was possible by using the relaxation time of Equation (20). But a good fit was accomplished by using Equation (19) with the resonant frequencies ω_{o1} and ω_{o2}, 9.04 and 11.13 cm^{-1} respectively. Then different values of δ and D, the mean parameter in the Fletcher and Stevens model (6) were tested looking for transitions of the order of the resonants energies, ω_{o1} and ω_{o2}, that fitted the λ/T^3 data. In finding these transitions energies only energy levels of reasonable population were considered. These energy level populations were calculated from the Boltzman distribution for phonons

$$f_i = \frac{g_i \exp(-\varepsilon_i/KT)}{\sum_j g_j \exp(-\varepsilon_j/KT)} \qquad (21)$$

where f_i is the population of the ith level and ε_i its energy; g_i is the level degeneracy and j runs over all states.

It was found that values of δ = 10.6 cm^{-1}, and D = 0.93 cm^{-1} reproduced the resonance energies 9.04 and 11.13 cm^{-1} corresponding to the transitions $E_1 \rightarrow A_2$ and $E_1 \rightarrow E_2$ respectively. These values for δ and D are in excellent agreement with the values found by Lange and Guha (9).

Tabulation of some values of the energy levels for various choices of δ and D are presented in Appendix H, and the corresponding transition energies in Appendix I. The energy level scheme that fit the data of samples B and C is shown in Figure 10, and the tabulation of the fitting parameters are in Table IV.

TABLE IV

FITTING PARAMETERS FOR THE DOPED SAMPLES

Sample	Boule	ΔA (10^{-44} Sec^3)	B_1 (10^{31} Sec^{-3})	ω_{o1} (cm^{-1})	B_2 (10^{31} Sec^{-3})	ω_{o2} (cm^{-1})
B	081374	1.6	7.732	9.04	6.185	11.13
C	022475	2.1	19.33	9.04	15.46	11.13

It is expected that the $E_2 \rightarrow A_1$ resonant transition can be observed if the thermal conductivity measurements are extended to lower temperatures.

In performing the fitting of the experimental data the ratio B_1/B_2 was kept constant for both doped samples, which suggests that both the resonant scatterings are due to the same ion or defect.

The solid lines in Figure 4 correspond to the fitted data, using the parameters of Table IV.

The Rayleigh scattering parameter was one order of magnitude higher in the doped samples than in the pure sample. The ratio of these para-

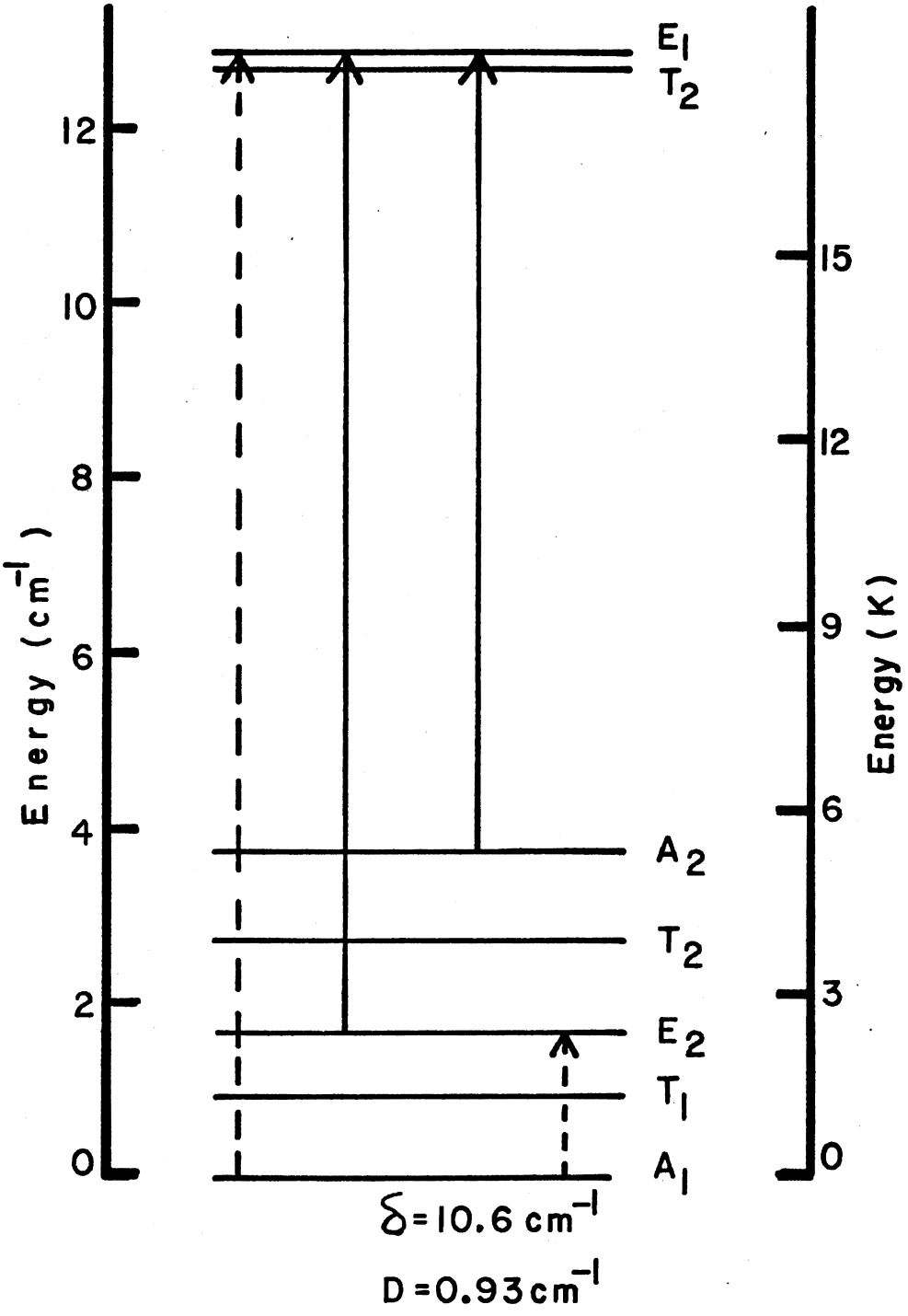

Figure 10. Energy Level Diagram for Cr^{2+} in $KMgF_3$ Including the Jahn-Teller Effect

meters for the doped samples was 1.3 that is into the order of magnitude of the concentration of chromous impurities in the samples, taking account that the accuracy of the concentration determination was of ±20%.

Summary

Thermal conductivity measurements on samples of potassium magnesium fluoride were independent of the direction of the heat flow.

The Debye-Callaway model for thermal conductivity turned to be a consistent way to fit the experimental data for all samples.

The data for the doped samples showed that the paramagnetic chromous ions interact strongly with phonons. The thermal conductivity was reduced considerably on the doped samples, at low temperatures. Two resonances were found on the conductivities of these samples.

The resonant energies that fitted the thermal conductivity data for the doped samples were consistent with the dynamical Jahn-Teller effect theory of Fletcher and Stevens for octahedrally co-ordinated $3d^4$ ions (6). The values found for the parameters δ and D of this model were in excellent agreement with the values found by Lange and Guha (9) to account for their acoustic paramagnetic data on samples from the same boule of sample B on this experiment.

A SELECTED BIBLIOGRAPHY

1. Orbach, R. "Thermal Resistance of Holmium Ethyl Sulfate." Phys. Rev. Lett., 8 (1962), 393-396.

2. Walker, C. T. and R. O. Pohl. "Phonon Scattering by Point Defects." Phys. Rev., 131 (1963), 1433-1442.

3. Walton, D. "Phonon Scattering by Paramagnetic Ions and Scattering by Other Defects." Phys. Rev., 151 (1966), 627-628.

4. Walton, D. "Study of the Li Ion in KCl Using the Spin-Phonon Interaction." Phys. Rev. Lett., 19 (1967), 305-307.

5. Jahn, H. A. and E. Teller. "Stability of Polyatomic Molecules in Degenerate Electronic States." Proc. Roy. Soc. A, 161 (1937), 220-235.

6. Fletcher, J. R. and K. W. H. Stevens. "The Jahn-Teller Effect of Octahedrally Co-ordinated $3d^4$ Ions." J. Phys. C., 2 (1969), 444-456.

7. Challis, L. J., et al. "In Investigation of the Ground State of Cr^{2+} in MgO Based on Thermal Conductivity Measurements." Proc. R. Soc. Lond. A, 330 (1972), 29-58.

8. Lange, J. N. "Dynamic Jahn-Teller Effect for Cr^{2+} in MgO: Hypersonic Attenuation." Phys. Rev. B, 12 (1973), 5999-6009.

9. Lange, J. N. and S. Guha. "Temperature Dependence of the Acoustic Paramagnetic Resonance Spectra for Cr^{2+} in MgO and $KMgF_3$." Phonon Scattering in Solids. Ed. L. J. Challis, V. W. Rampton and A. F. G. Wyatt. New York: Plenum Press, 1976, pp. 175-177.

10. Wyckoff, R. W. G. Crystal Structures. Vol. 2, Ed. Interscience Publishers. New York: John Wiley & Sons, 1967.

11. Rosenberg, H. M. and J. K. Wigmore. "The Elastic Constants of Potassium Magnesium Fluoride." Phys. Lett. A, 6 (1967), 317.

12. Harley, R. T. and H. M. Rosenberg. "The Thermal Conductivity of Ni^{2+} Doped $KMgF_3$ in a Magnetic Field at Low Temperatures: the Effect of Single Ions and Coupled Pairs." Proc. Soc. Lond. A, 315 (1970), 551-569.

13. Wolf, Michael W. "The Low Temperature Thermal Conductivity of Potassium Zinc Fluoride." (Unpub. Ph.D. Dissertation, Oklahoma State University, 1974.)

14. Callaway, Joseph. "Model for Lattice Thermal Conductivity at Low Temperature." Phys. Rev., 113 (1959), 1046-1051.

15. Challis, L. J., M. A. McConachie, and D. J. Williams. "An Investigation of Phonon Scattering by Chromous Ions in MgO by Thermal Conductivity Measurements." Proc. Roy. Soc. A, 308 (1968), 355-376.

16. Pohl, R. O. "The Applicability of the Debye Model to Thermal Conductivity." Zeitschrift für Physik, 176 (1963), 358-369.

17. Carruthers, P. "Theory of Thermal Conductivity of Solids at Low Temperatures." Revs. Modern Phys., 33 (1961), 92-138.

18. Baumann, F. C., et al. "Thermal Conductivity in Mixed Alkali Halides:KCl:Li and KBr:Li." Phys. Rev., 159 (1967), 691-699.

19. Casimir, H. B. G. "Note on the Conduction of Heat in Crystals." Physica, 5 (1938), 495-500.

20. Klemens, P. G. "Thermal Conductivity and Lattice Vibrational Modes." Solid State Physics. Vol. 7, Ed. F. Seitz. New York: Academic Press, 1958, pp. 1-98.

21. Klemens, P. G. Encyclopedia of Physics. Vol. 14, Ed. S. Fugge. Berlin: Springer-Verlog, 1956.

22. Slack, G. A. "Thermal Conductivity of MgO, Al_2O_3, $MgAl_2O_4$, and Fe_3O_4 Crystals From 3 to 300K." Phys. Rev., 126 (1962), 427-441.

23. Slack, G. A. and S. Galginaitis. "Thermal Conductivity and Phonon Scattering by Magnetic Impurities in CdTe." Phys. Rev. A, 133 (1964), 253-268.

24. Holland, M. G. "Analysis of Thermal Conductivity." Phys. Rev., 132 (1963), 2461-2471.

25. Pohl, R. O. Localized Excitations in Solids. Ed. R. F. Wallis. New York: Plenum Press, 1968.

26. Sheard, F. W. "Spin Phonon Interaction." Phonon Scattering in Solids. Ed. L. J. Challis, V. W. Rampton and A. F. G. Wyatt. New York: Plenum Press, 1976, pp. 154-162.

27. Griffin, A. and P. Carruthers. "Thermal Conductivity of Solids IV: Resonance Fluorescence Scattering by Donor Electrons in Germanium." Phys. Rev., 131 (1963), 1976-1995.

APPENDIX A

TABULATION OF DATA FOR SAMPLE A

($KMgF_3$:UNDOPED)

2.5 TO 80K

Temperature (K)	Thermal Conductivity (mW/cm K)
2.5	207.5
2.8	252.0
3.2	413.0
3.4	389.9
3.7	690.0
4.2	799.1
4.5	1124.6
4.9	1422.6
5.6	1804.4
6.6	2849.6
6.8	2989.2
8.0	4112.8
9.0	4740.8
10.0	5955.3
11.1	6619.2
12.6	7299.7
14.0	8088.9
15.0	9525.2
17.3	9003.9
20.0	7862.9
23.0	4939.7
25.0	3613.4
79.0	360.2
79.2	345.7
79.3	359.8
80.0	328.0

APPENDIX B

TABULATION OF DATA FOR SAMPLE A1

($KMgF_3$:UNDOPED)

3.8 TO 79.5 K

Temperature (K)	Thermal Conductivity (mW/cm K)
3.8	460.8
4.2	612.1
5.2	1174.2
7.0	2264.0
8.6	3265.4
10.0	4214.6
79.3	320.0
79.5	317.0

APPENDIX C

TABULATION OF DATA FOR SAMPLE B

($KMgF_3$:CHROMOUS 2^+ DOPED)

2.3 TO 81.0 K

Temperature (K)	Thermal Conductivity (mW/cm K)
2.3	17.3
2.5	21.5
2.8	29.1
3.1	39.6
3.4	53.7
3.8	72.8
4.1	97.1
4.2	105.9
4.3	113.4
4.4	120.1
4.5	135.0
4.5	136.7
4.7	157.6
4.9	202.9
5.1	202.6
5.3	223.7
5.6	284.5
6.0	366.4
6.5	471.2
7.0	592.3
8.0	850.0
9.0	1125.0
10.0	1443.9
12.0	2029.5
14.0	2661.4
15.0	2869.2
17.0	3151.2
18.5	3346.0
25.0	2462.1
46.1	799.6
50.0	737.9
53.4	668.5

APPENDIX C (Continued)

Temperature (K)	Thermal Conductivity (mW/cm K)
64.7	531.9
77.4	461.4
77.9	428.3
78.1	422.8
81.1	391.7
81.1	397.4

APPENDIX D

TABULATION OF DATA FOR SAMPLE C

($KMgF_3$:CHROMOUS 2^+ DOPED)

2.4 TO 152K

Temperature (K)	Thermal Conductivity (mW/cm K)
2.4	10.3
2.6	11.8
2.9	15.4
3.2	21.1
3.4	25.4
3.7	31.2
3.7	34.6
3.8	37.5
3.9	40.0
4.2	44.0
4.5	73.1
4.7	86.4
4.8	98.5
4.9	108.6
5.0	108.0
5.2	124.6
5.3	139.5
5.8	201.8
6.6	302.6
7.4	437.2
8.3	612.1
9.7	910.4
12.1	1401.9
14.0	1831.7
16.7	2275.1
18.0	2361.0
20.0	2316.3
22.5	2074.0
24.2	1952.4
28.0	1639.2
33.3	1224.1
45.7	1493.6
45.9	1543.0

APPENDIX D (Continued)

Temperature (K)	Thermal Conductivity (mW/cm K)
46.0	1491.6
49.0	1261.9
54.9	936.1
59.8	783.3
63.8	716.9
66.8	674.6
69.8	626.6
77.7	551.2
77.7	542.0
77.8	520.2
78.0	445.6
78.3	414.4
86.3	446.9
98.5	371.2
119.0	293.3
152.5	213.4

APPENDIX E

TABULATION OF DATA FOR SAMPLE D

($KMgF_3$:CHROMOUS 2^+ DOPED)

5.2 TO 153K

Temperature (K)	Thermal Conductivity (mW/cm K)
5.3	133.3
5.6	176.0
6.0	233.0
6.5	299.5
7.0	371.2
7.5	465.3
8.6	633.4
10.0	925.0
12.0	1272.7
13.7	1522.0
15.1	1839.6
17.9	2205.4
21.1	2229.9
25.2	1668.6
34.2	1139.9
48.2	711.6
52.3	676.4
55.6	632.2
58.2	540.2
61.9	520.6
65.0	521.0
71.5	462.1
77.3	449.6
77.5	441.3
78.1	453.0
78.2	457.4
78.8	414.4
85.0	397.6
85.1	398.5
98.5	345.1
99.0	304.2
121.0	245.4
124.5	262.7
153.5	207.5

APPENDIX F

THE CALCULATION OF THE PARAMETERS Γ OF EQUATION 13 FOR ISOTOPE POINT DEFECT SCATTERING IN $KMgF_3$

$$\Gamma = \frac{1}{5}\left(\frac{\bar{M}_K}{\bar{M}}\right)^2 \Gamma_K + \frac{1}{5}\left(\frac{\bar{M}_{Mg}}{\bar{M}}\right)^2 \Gamma_{Mg} + \frac{3}{5}\left(\frac{\bar{M}_F}{\bar{M}}\right)^2 \Gamma_F$$

$$= \frac{1}{5}\left(\frac{39.1}{24.08}\right)^2 \Gamma_K + \frac{1}{5}\left(\frac{24.32}{24.08}\right)^2 \Gamma_{Mg} + \frac{3}{5}\left(\frac{19}{24.08}\right)^2 \Gamma_F$$

$$= 2.408 \times 10^{-4}$$

where

$$\Gamma_K = \sum_i f_{K_i}\left(\frac{\Delta M_{K_i}}{\bar{M}_K}\right) \text{ with } i = 39,40,41$$

$$= (0.931)\left(\frac{0.102}{39.1}\right)^2 + (1.18 \times 10^{-4})\left(\frac{0.898}{39.1}\right)^2$$

$$+ (0.0688)\left(\frac{1.89}{39.1}\right)^2$$

$$= 1.671 \times 10^{-4}$$

$$\Gamma_{Mg} = \sum_i f_{Mg_i} \left(\frac{\Delta M_{Mg_i}}{\bar{M}_{Mg}}\right)^2 \quad \text{with } i = 23.9,\ 24.9,\ 25.9$$

$$\Gamma_{Mg} = (0.781)\left(\frac{0.327}{24.31}\right)^2 + (0.101)\left(\frac{0.674}{24.31}\right)^2 + (0.112)\left(\frac{1.671}{24.31}\right)^2$$

$$= 7.486 \times 10^{-4}$$

$$\Gamma_F = \sum_i f_{F_i} \left(\frac{\Delta M_{F_i}}{\bar{M}_F}\right)^2 \quad \text{with } i = 19$$

$$= (1.0)\left(\frac{1.6 \times 10^{-3}}{19}\right)^2 = 7.1 \times 10^{-9}$$

APPENDIX G

ENERGY LEVELS OF THE GROUND STATE OF AN OCTAHEDRICALLY CO-ORDINATED $3d^4$ ION FROM THE JAHN-TELLER EFFECT MODEL OF FLETCHER AND STEVENS

For B > O

B is the anharmonic constant and can be positive or negative.

$$A_1 = -\frac{\delta}{3} - 2 f_1 D$$

$$A_2 = -\frac{\delta}{3} + 2 f_1 D$$

$$E_1 = \frac{\delta}{6} + \left(\frac{\delta^2}{4} + 2 f_2^2 D^2\right)^{\frac{1}{2}}$$

$$E_2 = \frac{\delta}{6} - \left(\frac{\delta^2}{4} + 2 f_2^2 D^2\right)^{\frac{1}{2}}$$

$$T_1 = -\frac{\delta}{3} - f_1 D$$

$$T_2 = \frac{\delta}{6} + f_1 \frac{D}{2} + \left\{\frac{(\delta - f_1 D)^2}{4} + f_2^2 D^2\right\}^{\frac{1}{2}}$$

$$T_2' = \frac{\delta}{6} + f_1 \frac{D}{2} - \left\{\frac{(\delta - f_1 D)^2}{4} + f_2^2 D^2\right\}^{\frac{1}{2}}$$

f_1 and f_2 are factors that arise from the spin degeneracy. They are

slowly functions of δ, and were determined and tabulated by Fletcher and Stevens (6). In this work values of $f_1 = 1.0$ and $f_2 = 1.2$ were used. These are appropriate to the large value of δ required by the data. These same values were also used by Lange and Guha (9).

APPENDIX H

SAMPLE VALUES OF ENERGY LEVELS IN CM^{-1} FROM THE FLETCHER AND STEVENS MODEL

δ	D	A_1	T_1	E_2	T_2'	A_2	T_2	E_1
6.0	1.0	- 4.0	-3.0	-2.4	-1.3	0	4.3	4.4
8.0	2.0	- 6.7	-4.7	-3.9	-1.5	1.3	6.2	6.6
10.0	2.5	- 8.3	-5.8	-4.9	-1.9	1.7	7.7	8.2
10.67	0.93	- 5.4	-4.5	-3.8	-2.7	-1.7	7.2	7.3
12.0	0.5	- 5.0	-4.5	-4.1	-3.5	-3.0	12.3	13.1
16.0	4.0	-13.3	9.3	-7.8	-3.0	2.6	8.0	8.1

APPENDIX I

SAMPLE VALUES OF TRANSITION ENERGIES IN CM^{-1}

FROM THE FLETCHER AND STEVENS MODEL

δ	D	E_2-A_1	E_1-A_1	A_2-E_2	E_1-E_2	E_1-A_2	$T_2'-T_1$	T_2-T_1	T_2-T_2'
6.0	1.0	1.5	8.4	2.4	6.9	4.4	1.7	7.3	5.5
8.0	2.0	2.7	13.2	5.2	10.5	5.2	3.2	10.8	7.7
10.0	2.5	3.4	16.5	6.5	13.1	6.5	3.9	13.5	9.6
10.67	0.93	1.6	12.7	2.1	11.1	9.0	1.7	11.7	10.0
12.0	0.5	0.9	13.0	1.1	12.1	11.1	1.0	12.5	11.6
16.0	4.0	5.5	26.5	10.5	21.0	10.5	6.3	21.7	15.4

VITA

Augusto R. Lopez

Candidate for the Degree of

Doctor of Philosophy

Thesis: LOW TEMPERATURE THERMAL CONDUCTIVITY OF $KMgF_3:Cr^{2+}$

Major Field: Physics

Biographical:

Personal Data: Born in Santa Marta, Magdalena, Colombia, August 5, 1939, the son of Don Bernardo Lopez Morales and Doña Urania Z. de Lopez.

Education: Graduated from Escuela Normal del Atlantico, Barranquilla, Colombia, in November 1957; received Licenciado degree in Mathematics and Physics from Universidad Pedagogica y Technologica de Colombia in 1962; received Master of Science degree in Physics from Emporia Kansas State College in 1969; attended graduate summer school at University of Notre Dame in a program sponsored by the Organization of American States and the National Science Foundation, 1972; completed requirements for the Doctor of Philosophy degree at Oklahoma State University in July, 1976.

Professional Experience: Sciences professor, Colegio Nacional Academico, Cartago, Colombia, 1962-63; Mathematics and Physics professor, Liceo Celedon, Santa Marta, Colombia, 1963-65; Physics professor, Universidad del Atlantico, Barranquilla, Colombia, 1965-67; Physics professor, Universidad Industrial de Santander, Bucaramanga, Colombia, 1968-73; graduate teaching assistant, Oklahoma State University, Department of Physics, 1973-76.

Organizations: Member of Sigma Pi Sigma, American Association of Physics Teachers, Sociedad Colombiana de Fisica.